

**A highly fluorinated lithium iron phosphate with interpenetrating lattices:**

**Electrochemistry and Ionic conductivity**

Hooman Yaghoobnejad Asl,<sup>a</sup> Kartik Ghosh<sup>b</sup> and Amitava Choudhury<sup>a,\*</sup>

<sup>a</sup>Department of chemistry, Missouri University of Science and Technology, Rolla, MO 65409,

USA

<sup>b</sup>Department of Physics, Astronomy, and Materials Science and the Center for Applied Science and Engineering, Missouri State University, Springfield, Missouri 65897, United States

Serial Number	Contents	Page Number
Figure S1	Cycle life testing of $\text{Li}_5\text{Fe}_2(\text{PO}_4)\text{F}_8$ as cathode	S2
Figure S2	GITT curves for $\text{Li}_5\text{Fe}_2(\text{PO}_4)\text{F}_8$	S3
Figure S3	TGA curve of $\text{Li}_5\text{Fe}_2\text{PO}_4\text{F}_8$	S4
Figure S4	Arrhenius plot of $\text{Li}^+$ diffusivity vs. temperature	S5
Table S1	Atomic coordinates and thermal displacement parameters for $\text{Li}_5\text{Fe}_2\text{PO}_4\text{F}_8$ .	S6
Table S2	Distortion analysis of polyhedra	S7

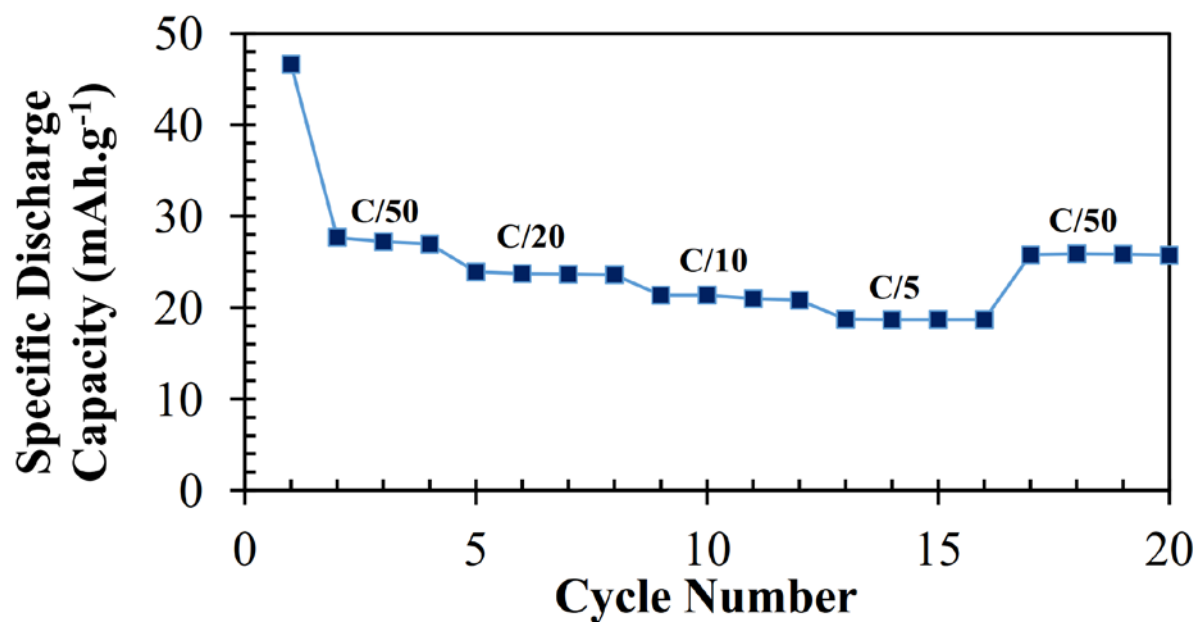


Figure S1: Test of cycle life showing capacity retention at various C-rates for  $\text{Li}_5\text{Fe}_2(\text{PO}_4)\text{F}_8$  cathode.

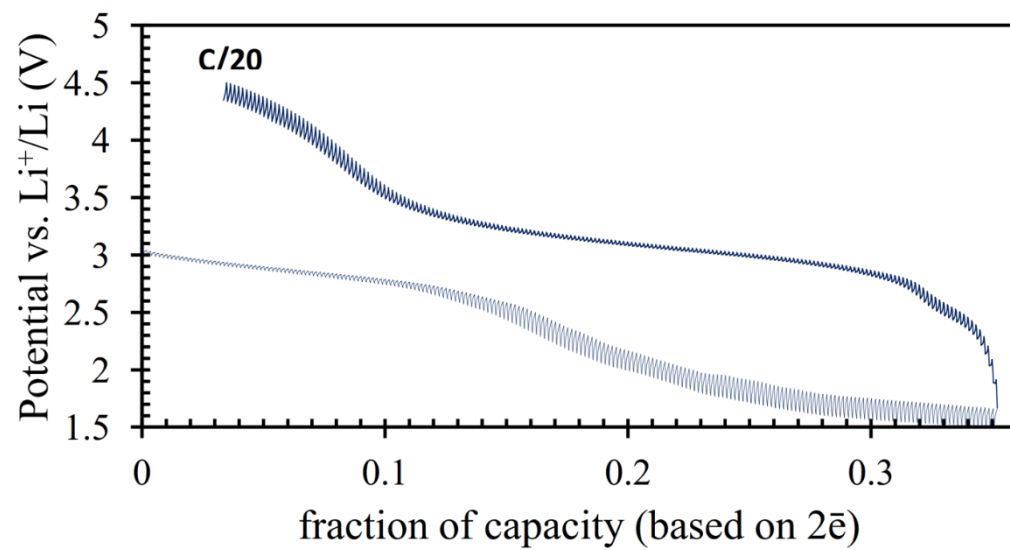


Figure S2. Charge-discharge GITT curves for  $\text{Li}_5\text{Fe}_2(\text{PO}_4)\text{F}_8$

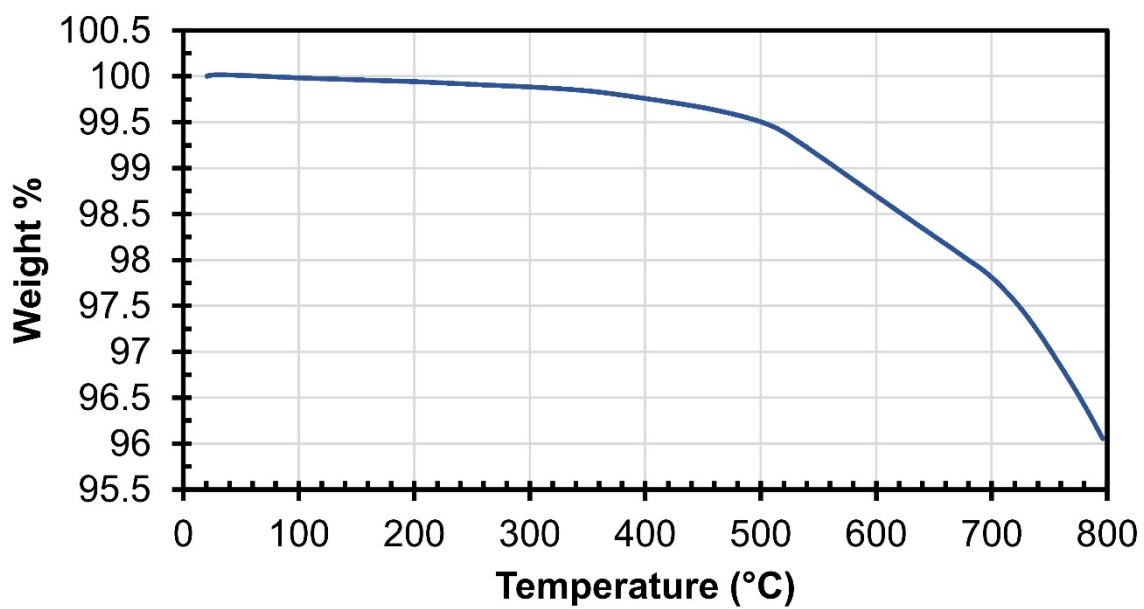


Figure S3. TGA curve of  $\text{Li}_5\text{Fe}_2\text{PO}_4\text{F}_8$  under  $\text{N}_2$  flow at  $10\text{ }^\circ\text{C}\cdot\text{min}^{-1}$  heating rate.

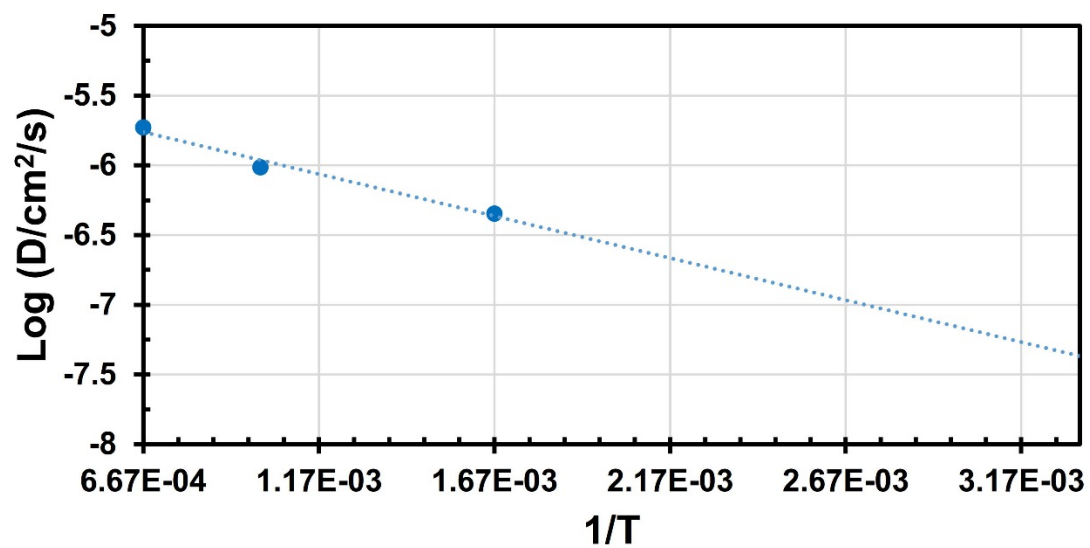


Figure S4. Arrhenius plot of Li<sup>+</sup> diffusivity vs. temperature as obtained from ab initio molecular dynamic (AIMD) simulations.

Table S1. Atom list, fractional coordinates and isotropic thermal displacement parameters for  $\text{Li}_5\text{Fe}_2\text{PO}_4\text{F}_8$ .  $U_{\text{eq}} = 1/3^{\text{rd}}$  of the trace of the orthogonalized U tensor.

Atom	Wyck.	Occ.	x/a	y/b	z/c	U [ $\text{\AA}^2$ ]
Fe1	8f	1.00	0.37601(2)	0.51532(4)	0.27215(4)	0.0083(1)
Fe2	4d	1.00	0.25	1.00	-0.04605(5)	0.0087(1)
Fe3	4a	1.00	0.25	1.00	0.00	0.0083(1)
P1	8f	1.00	0.37435(3)	0.74656(7)	0.00677(6)	0.0071(1)
O1	8f	1.00	0.31682(9)	0.83157(8)	-0.07309(7)	0.0120(3)
O2	8f	1.00	0.33937(8)	0.65843(7)	0.12638(7)	0.0104(3)
O3	8f	1.00	0.42926(8)	0.85150(8)	0.07129(7)	0.0100(3)
O4	8f	1.00	0.41226(8)	0.64232(8)	-0.09649(6)	0.0094(3)
F1	8f	1.00	0.44384(7)	0.64609(1)	0.35583(3)	0.0140(3)
F2	8f	1.00	0.44287(7)	0.43440(6)	0.14193(4)	0.0136(3)
F3	8f	1.00	0.54925(7)	0.85730(1)	-0.12015(6)	0.0131(3)
F4	8f	1.00	0.30643(7)	0.38820(3)	0.19217(4)	0.0143(3)
F5	8f	1.00	0.30977(7)	0.59885(2)	0.40567(7)	0.0141(3)
F6	8f	1.00	0.55805(7)	0.94338(6)	0.15107(4)	0.0143(3)
F7	8f	1.00	0.30736(7)	1.10281(8)	0.09011(6)	0.0158(3)
F8	8f	1.00	0.30515(7)	1.09828(7)	-0.18947(6)	0.0145(3)
Li1	4e	1.00	0.25	0.50	0.5506(7)	0.0201(4)
Li2	4b	1.00	0.50	0.50	0.00	0.0291(8)
Li3	8f	1.00	0.6239(2)	1.0111(6)	0.2834(5)	0.0218(1)
Li4	4c	1.00	0.50	0.7893(7)	0.25	0.0181(3)
Li5	4c	1.00	0.50	0.7160(8)	-0.25	0.0231(3)
Li6	8f	1.00	0.2460(3)	0.2546(7)	0.2584(7)	0.0367(6)
Li7	8f	1.00	0.3765(3)	0.7436(9)	0.5112(9)	0.060(3)

Table S2. Polyhedral details and distortion analysis for the three crystallographically unique iron sites in  $\text{Li}_5\text{Fe}_2\text{PO}_4\text{F}_8$ .

	Fe1	Fe2	Fe3
Average bond length ( $\text{\AA}$ )	1.9570	1.9584	1.9558
Polyhedral volume ( $\text{\AA}^3$ )	9.8999	9.8986	9.9272
Distortion index (bond length)	0.02412	0.01769	0.02716
Quadratic elongation	1.0070	1.0081	1.0042
Bond angle variance ( $^\circ^2$ )	19.4884	25.3239	8.0046
Effective C.N.	5.8539	5.9258	5.7554